Available online at www.sciencedirect.com
ScienceDirect
Earth and Planetary Science Letters 261 (2007) 491–499
EPSL
www.elsevier.com/locate/epsl

Pu–Xe, U–Xe, U–Pb chronology and isotope systematics of ancient zircons from Western Australia

Grenville Turner [a,*], Alli Busfield [a], Sarah A. Crowther [a], Mark Harrison [b], Stephen J. Mojzsis [c], Jamie Gilmour [a]

[a] *SEAES, University of Manchester, UK*
[b] *Department of Earth and Space Science, UCLA, CA 90095, USA*
[c] *Department of Geological Sciences, University of Colorado, Boulder, Colorado 80309-0399, USA*

Received 26 March 2007; received in revised form 9 July 2007; accepted 9 July 2007
Available online 18 July 2007
Editor: R.W. Carlson

Abstract

The presence of xenon isotopes from in-situ spontaneous fission of short-lived ^{244}Pu has been confirmed in a suite of 16 Hadean detrital zircons from Western Australia. In order to investigate the effects of xenon loss on estimates of the inferred Pu/U ratio we have irradiated the zircons with thermal neutrons to generate Xe from ^{235}U neutron fission. ^{131}Xe/^{134}Xe and ^{132}Xe/^{134}Xe ratios have been used to calculate the relative contributions from spontaneous fission of ^{244}Pu and ^{238}U and neutron fission of ^{235}U and hence compare nominal Pu/U ratios and xenon retention ages. U–Xe ages are typically lower than the Pb–Pb ages, indicating that xenon loss is common. We show how the ternary mixing diagram can be used to place constraints on the timing and extent of this loss and to generate a corresponding Pu–U–Xe isochron. Although the zircons investigated in this study were extracted from the same metasedimentary unit, the timing of xenon loss is variable. This suggests that the loss may be the result of variable degrees of metamictization from grain to grain. Inferred $(Pu/U)_o$ ratios show a general decrease with the discordancy between Pb–Pb and U–Xe ages. For the least discordant samples we infer $(Pu/U)_o \sim 0.008$ which is close to the widely adopted chondritic value. While we cannot completely exclude the effects of Pu/U fractionation in magmatic and other processes between formation of the Earth and crystallisation of the zircons we conclude that they have been relatively small (< factor 2?) and reflect the compatible behaviour of Pu and U in the 4+ valence state.

Keywords: ^{244}Pu; xenon; Pu–Xe; U–Xe; zircon; Hadean; Pu/U; isotope; chronology; fission

1. Introduction

With a half-life of 82 Ma, ^{244}Pu is one of the longest lived of the so-called extinct isotopes that were present in the early solar system and which record nucleosynthetic processes immediately preceding its formation. The initial ^{244}Pu/^{238}U ratio of the solar system, hereafter abbreviated to $(Pu/U)_o$, is an important parameter in models of nucleosynthesis, cosmochronology (e.g. Lugmair and Marti, 1977; Clayton, 1983; Hudson et al., 1989; Wasserburg et al., 1996; Meyer and Clayton, 2000) and of the development of the terrestrial mantle and atmosphere (Staudacher and Allègre, 1982;

* Corresponding author.
E-mail address: grenville.turner@manchester.ac.uk (G. Turner).

0012-821X/$ - see front matter © 2007 Elsevier B.V. All rights reserved.
doi:10.1016/j.epsl.2007.07.014

O'Nions and Tolstikhin, 1994; Porcelli and Wasserburg, 1995; Kunz et al., 1998). We previously reported evidence, in the form of fissiogenic xenon isotopes, for in situ decay of ^{244}Pu in individual 4.1–4.2 Ga zircons from the Jack Hills region of Western Australia (Turner et al., 2004). The $(Pu/U)_o$ inferred from these results varied from essentially zero to 0.007 (since revised to 0.008: Turner et al., 2005) for individual zircons. Since that work we have attempted to develop an understanding of the factors responsible for this variation, specifically; the extent and timing of post-crystallization fissiogenic xenon loss, and the geochemical behaviour of plutonium in early magmatic processes. Here we report results from a larger suit of zircons designed to address these questions.

Because our previous analyses relied exclusively on xenon isotope ratios in the individual zircons we were unable to determine Xe/U ratios, which could provide evidence regarding xenon loss. In the present work we have attempted to overcome this deficiency by irradiating a suite of 16 zircons with thermal neutrons to generate Xe from ^{235}U neutron fission. ^{131}Xe/^{134}Xe and ^{132}Xe/^{134}Xe ratios can be used to calculate the relative contributions from spontaneous fission of ^{244}Pu and ^{238}U and neutron fission of ^{235}U and hence allow us to compare nominal Pu/U ratios and xenon retention ages.

2. Methodology

The use of neutron activation to determine xenon retention ages based on the spontaneous fission of ^{238}U is long established (Shukolyukov et al., 1974; Teitsma et al., 1975) and is analogous to the Ar–Ar method and its predecessor I–Xe dating. The use of the technique for zircons containing xenon from the spontaneous fission of ^{244}Pu is complicated by the need to disentangle three xenon components produced from fission of ^{238}U, ^{235}U and ^{244}Pu. The fissiogenic isotopes available to accomplish this are ^{131}Xe, ^{132}Xe, ^{134}Xe and ^{136}Xe. As usual, ^{130}Xe, which is shielded in fission, can be used to apply corrections for atmospheric xenon. In addition to neutron-induced fission of ^{235}U, ^{131}Xe is produced by (n,γ) reactions on ^{130}Ba. Fortunately the Ba/U ratio in zircons is small (average 0.006 in Jack Hills zircons; Peck et al., 2001) and the production of ^{131}Xe by this route can be ignored. ^{136}Xe, which would commonly be taken as the reference isotope when comparing fissiogenic components, is also produced by (n,γ) reactions on short-lived ^{135}Xe. Analysis of xenon produced in a uranium bearing glass indicates that this effect was negligible in the present irradiation. Nevertheless we have taken ^{134}Xe as reference isotope on account of the larger overall variation in ^{132}Xe/^{134}Xe compared to ^{132}Xe/^{136}Xe.

The Pu/U ratio recorded in the zircons may be determined from the ratio of ^{134}Xe produced by spontaneous fission of ^{244}Pu to that from spontaneous fission of ^{238}U. The corresponding lower limit to the $(Pu/U)_o$ ratio at solar system 'time zero' is calculated from the decay interval between 4.57 Ga and the Pb–Pb age of the zircon. Loss of xenon at some later time will lead to a lowering of the calculated $(Pu/U)_o$ ratio because of preferential loss of Pu–Xe due to the short half-life of ^{244}Pu in comparison to that of ^{238}U. Conversely an underestimation of the formation age of the zircon will raise the calculated $(Pu/U)_o$ ratio.

An alternative estimate of Pu/U may be obtained from the ratio of ^{134}Xe from spontaneous fission of ^{244}Pu to that from neutron induced fission of ^{235}U. In this case xenon loss affects the estimate of the ^{244}Pu abundance but not ^{235}U, leading to a lower estimate of Pu/U than that from the procedure described in the previous paragraph. Only in the case where no loss has occurred will the two estimates of (Pu/U) agree.

The U–Xe age of a zircon is calculated from the ratio of ^{134}Xe produced by spontaneous fission of ^{238}U to that from neutron-induced fission of ^{235}U. Where partial loss of fissiogenic xenon has occurred the U–Xe age will be intermediate between the formation age and the time of partial loss. Partial loss is evident in those cases where ^{244}Pu–Xe is present but the U–Xe age corresponds to a time after the complete decay of ^{244}Pu. The implications of this are central to the subsequent discussion.

The effects of recoil loss of xenon from zircons have been reported previously (Hebeda et al., 1987) with estimated recoil distances of around 10 μm. The detrital zircons we have analysed were roughly equidimensional with sizes in the range 200–300 μm, from which we estimate recoil losses of 1–2%. Moreover, to the extent that the energy spectra of the recoiling xenon atoms are comparable for the three parent nuclides, the effects of these recoil losses on the measured isotope ratios will tend to cancel. For these reasons we have chosen to ignore recoil.

3. Results

We have analysed 16 zircons (probe section ANU133) with Pb–Pb ages ranging from 3976 Ma to 4159 Ma. Individual zircons were step-heated to fusion using the fundamental wavelength of a Nd:YAG laser to release xenon. The gettered gas was analysed using the RELAX-1 resonance ionisation time-of-flight mass spectrometer (Gilmour et al., 1994). The xenon data for the major

release steps are shown in Table 1. Also listed in the table are the Pb–Pb and U–Pb ages, determined by ion microprobe. To test the effects of varying degrees of discordancy on Xe retention we included several zircons with highly discordant Pb–Pb and U–Pb ages. For the more imprecise analyses we list only an approximate Pb–Pb age. Note that one zircon, #6.4, had a 4.3 Ga core surrounded by a rim of zircon growth at 4.0 Ga.

Xenon data were corrected for mass discrimination, blank and for the contribution from atmospheric xenon using the observed ^{130}Xe. The atmospheric corrections become progressively inaccurate with increasing ^{130}Xe/^{134}Xe and extractions with ^{130}Xe/^{134}Xe greater than 0.01 have been ignored. The percentage correction to ^{134}Xe is indicated in the table.

All grains showed unambiguous evidence for fission xenon. Examination of the amount of gas released in each temperature step reveals a bimodal distribution with total xenon being dominated by a low temperature release and a smaller high temperature release. We do not have direct temperature estimates but a similar release pattern has been observed before for zircons (Krylov et al., 1993). In that work the lower temperature release peak occurred at 1330 °C to 1420 °C and the higher at 1480 °C to 1630 °C.

In order to determine the U–Xe age it is necessary to know the U to ^{134}Xe conversion factor for the irradiation.

Table 1
Atmosphere corrected Xe isotope ratios and age data[a] from zircons with uncorrected ^{130}Xe/^{134}Xe < 0.01

Sample	Laser Current	Atoms (/10^6)	^{134}Xe air (%)	^{131}Xe/^{134}Xe	^{132}Xe/^{134}Xe	^{136}Xe/^{134}Xe	Pb–Pb (Ma)	U–Pb (Ma)	U–Xe (Ma)	$(Pu/U)_o$ (/10^{-3})
1.4	13.0	3.50	−0.04(09)	0.165(02)	0.718(05)	1.112(04)	4005(12)	3802(45)	4240(190)	7.55(0.70)
	14.0	0.81	0.12(31)	0.170(07)	0.714(11)	1.119(08)			3700(370)	7.66(2.06)
	16.0	0.74	0.25(64)	0.176(14)	0.734(19)	1.119(12)			3910(790)	11.40(4.02)
1.7	13.5	2.22	0.10(12)	0.170(03)	0.714(05)	1.109(04)	4031(27)	3897(49)	3690(130)	6.25(0.62)
1.9	13.0	2.78	0.16(08)	0.168(02)	0.708(04)	1.114(04)	4126(17)	3804(51)	3640(120)	2.51(0.24)
	14.0	0.61	−0.07(97)	0.171(20)	0.712(28)	1.119(16)			3840(1020)	3.26(0.22)
	16.0	0.43	0.35(72)	0.193(16)	0.744(22)	1.087(14)			3010(770)	6.35(2.46)
2.8	13.0	0.78	1.60(50)	0.173(11)	0.710(15)	1.107(10)	*4013*		3410(430)	*7.42(3.14)*
2.14	12.0	0.56	0.27(57)	0.154(13)	0.665(17)	1.125(13)	4024(14)	3881(48)	3450(450)	0.57(1.87)
	12.5	2.69	0.00(09)	0.170(02)	0.693(04)	1.098(04)			3140(120)	4.21(0.57)
5.6	12.0	0.72	−0.58(38)	0.164(09)	0.693(12)	1.122(09)	4102(13)	3915(43)	3570(380)	2.17(0.87)
	13.0	3.39	0.13(08)	0.170(02)	0.712(03)	1.129(03)			3660(110)	3.38(0.29)
	14.0	3.30	0.20(10)	0.175(03)	0.723(05)	1.117(04)			3600(160)	4.45(0.41)
6.4	13.0	1.91	−0.01(15)	0.182(03)	0.710(06)	1.095(04)	*4000*		2830(120)	*9.29(1.10)*
	14.0	1.82	0.32(14)	0.181(03)	0.713(06)	1.098(04)			2970(130)	*9.67(1.12)*
7.2	12.0	1.06	0.14(28)	0.185(06)	0.718(10)	1.095(08)	4126(8)	3960(43)	2800(220)	4.02(0.84)
	13.0	0.47	1.04(46)	0.170(10)	0.718(16)	1.111(12)			3840(650)	3.13(1.17)
8.2	12.0	1.91	0.08(16)	0.181(04)	0.736(07)	1.113(06)	*4031*		3500(240)	*10.80(1.07)*
	13.0	0.66	0.18(51)	0.189(11)	0.766(16)	1.118(12)			4010(720)	*16.40(3.97)*
9.4	13.0	1.52	−0.02(18)	0.175(04)	0.691(07)	1.075(06)	4043(8)	4019(44)	2870(140)	3.75(0.82)
10.5	13.0	1.11	0.77(43)	0.158(09)	0.711(13)	1.139(09)	*4013*		4720(570)	*5.39(1.95)*
	14.0	0.98	1.35(27)	0.162(06)	0.726(10)	1.100(08)			4950(540)	*7.91(1.77)*
10.8	12.0	3.05	−0.21(10)	0.157(02)	0.668(04)	1.105(04)	4026(10)	4275(48)	3330(110)	0.74(0.47)
	13.0	0.38	0.43(66)	0.160(14)	0.652(21)	1.101(14)			2960(420)	−0.14(2.29)
	14.0	0.68	0.15(41)	0.154(09)	0.665(13)	1.107(09)			3470(310)	0.48(1.38)
	16.0	0.50	1.50(47)	0.147(10)	0.661(15)	1.104(11)			3850(390)	−0.43(1.42)
11.2	12.0	0.69	0.52(44)	0.160(10)	0.641(14)	1.088(10)	4159(10)	4183(44)	2760(250)	−0.58(0.50)
	13.0	1.98	−0.20(17)	0.178(04)	0.698(06)	1.110(05)			2880(150)	1.90(0.29)
12.12	12.0	2.00	0.02(15)	0.177(04)	0.739(05)	1.124(04)	4063(10)	3970(45)	3960(250)	7.80(0.65)
	14.0	1.33	1.74(31)	0.203(07)	0.775(10)	1.122(07)			3020(420)	16.90(2.80)
13.7	13.0	1.35	0.42(28)	0.176(06)	0.713(09)	1.112(07)	3976(8)	3940(53)	3300(290)	10.80(2.44)
14.5	12.0	0.50	−0.18(70)	0.150(16)	0.667(22)	1.159(16)	*3986*		3870(800)	*0.57(3.07)*
	13.0	5.95	−0.17(16)	0.190(04)	0.757(07)	1.099(06)			3450(270)	*21.20(1.95)*
	14.0	2.11	0.53(18)	0.187(04)	0.756(07)	1.124(06)			3660(230)	*20.60(2.13)*
	16.0	0.52	0.46(73)	0.210(16)	0.772(22)	1.100(13)			2510(690)	
^{244}Pu sf				0.262	0.942	1.065				
^{238}U sf				0.103	0.693	1.213				
^{235}U nf				0.320	0.560	0.819				

[a] 1σ errors on least significant figures are shown in brackets.

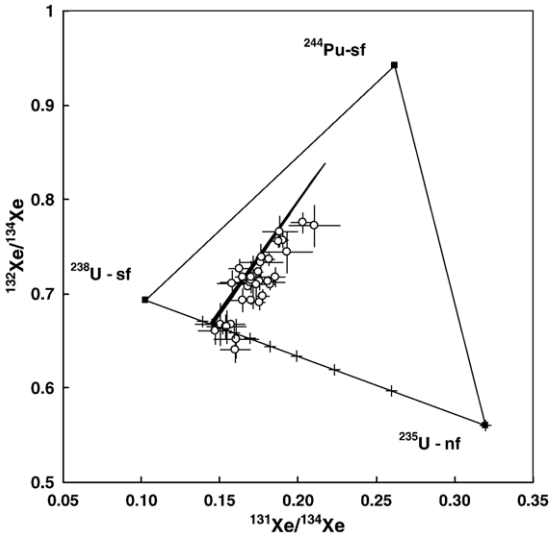

Fig. 1. Air corrected $^{132}Xe/^{134}Xe$ vs. $^{131}Xe/^{134}Xe$ ratios. The crosses indicate compositions of uranogenic xenon corresponding to U–Xe ages at 500 Ma intervals, increasing from zero at the ^{235}U end member. The solid lines represent a range of expected xenon compositions for zircons with ages in the range 3976 to 4159 Ma and $(Pu/U)_o$ ratios from zero to 0.016. Position of data points to the right of this line is indicative of xenon loss, a conclusion which is independent of $(Pu/U)_o$.

We irradiated and analysed 4 chips of NIST 610 which contains 461 ppm U. The xenon analyses were spiked with a known volume of ^{128}Xe to obtain the absolute quantity of excess ^{134}Xe in each chip and hence to derive the U to ^{134}Xe conversion factor, which we calculate to be 7.61×10^{-9}. This value is in excellent agreement with a value of 7.63×10^{-9} based on the neutron fluence measured by the team at the Imperial College Reactor Centre, London. The amount of uranium in each zircon is then calculated using this conversion factor and the measured ^{235}U-derived ^{134}Xe. The isotopic composition of the reactor produced xenon in the uranium glass was slightly different from literature values, which we presume to be a function of differences in the neutron spectrum.

Following air correction the data fall within the ^{244}Pu–^{238}U–^{235}U mixing triangle on a graph of $^{132}Xe/^{134}Xe$ against $^{131}Xe/^{134}Xe$ (Fig. 1). The $^{132}Xe/^{134}Xe$ and $^{131}Xe/^{134}Xe$ ratios have been used to resolve the contributions of the three end members in each temperature step, using the end member compositions listed at the foot of Table 1. The calculated contribution of each end member allows determination of the Pu/U ratio and U–Xe age recorded by each temperature release; these are also given in Table 1. The U–Xe ages typically range between 2500 and 4200 Ma. Comparison with the Pb–Pb ages indicates that xenon loss has occurred in many cases. As pointed out above, retention of ^{244}Pu fission xenon in zircons with low U–Xe ages implies that loss must have been incomplete and therefore have occurred more recently than the nominal U–Xe age.

Errors in the measured Pu/U ratio and U–Xe age and other quantities derived later are calculated using a Monte Carlo simulation technique and are based on 1σ instrumental errors. To achieve this we repeatedly produce a simulated, normally distributed, data set within the limits of the measured instrumental errors. The final value and error of derived quantities are obtained from the average and standard deviation of 100 simulations of the data set.

In Fig. 1 the U–Xe age is represented by the projection from the ^{244}Pu end-member to the 'age axis' which connects the ^{238}U and ^{235}U end-members. Crosses on this age axis indicate U–Xe ages increasing in increments of 500 Ma, from zero at the ^{235}U fission composition (i.e. zero ^{238}U fission xenon). The cluster of solid lines in Fig. 1 corresponds to the expected trajectory of the analytical data for U–Xe ages in the range 3976 to 4159 Ma and a range of $(Pu/U)_o$ ratios from 0 to 0.016, i.e. the case where the U–Xe ages and Pb–Pb ages agree. The observation that much of the actual data lies to the right of this line of concordancy illustrates graphically that xenon loss has occurred and that this conclusion is independent of the $(Pu/U)_o$ ratio.

In attempting to interpret the observed xenon compositions in more detail we are faced with three

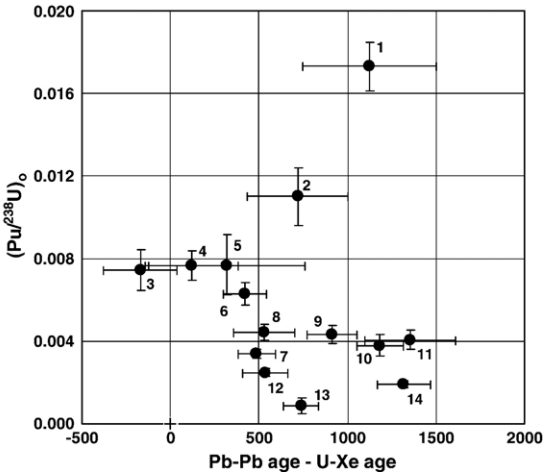

Fig. 2. Graph of $(Pu/U)_o$ against discordancy in Pb–Pb age and U–Xe age for samples with errors in ($^{131}Xe/^{134}Xe$) less than 5%. Aside from one high value (for the small high temperature release from 12.12) there is a general downward trend in $(Pu/U)_o$ with discordancy. The most concordant measurements correspond to $(Pu/U)_o$ similar to estimates from meteorites. Key to sample numbers and temperature steps shown in Table 1: 1—12.12(14), 2—13.7(13), 3—1.4(13), 4—12.12(12), 5—1.4(14), 6—1.7(13.5), 7—5.6(13), 8—5.6(14), 9—2.14(12.5), 10—9.4(13), 11—7.2(12), 12—1.9(13), 13—10.8(12), 14—11.2(13).

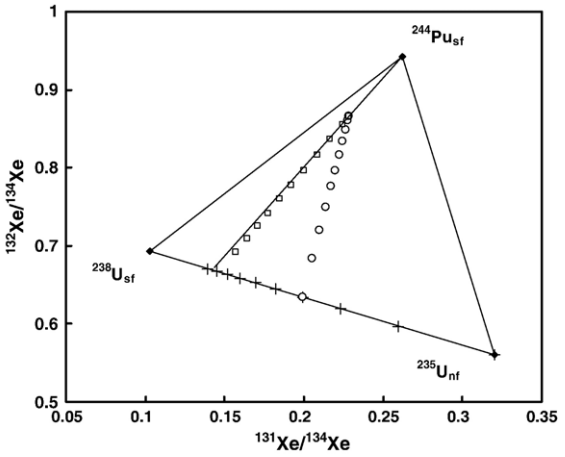

Fig. 3. $^{132}Xe/^{134}Xe$ vs. $^{131}Xe/^{134}Xe$ ratios showing theoretical isochrons for a 4200 Ma zircon partially outgassed to varying amounts at 3900 Ma (squares) and 1500 Ma (circles). The crosses indicate U–Xe ages at 500 Ma intervals increasing from zero at the ^{235}U end member. The solid line represents a concordant xenon mixing line corresponding to 4200 Ma. The starting point for the isochrons corresponds to a $(Pu/U)_o$ ratio of 0.008.

unknowns: The Pu/U ratio at a given epoch is unknown and moreover may vary between zircons of the same epoch as a result of Pu–U fractionation. The timing of xenon loss and the extent of that loss are also unknown. The present data set is sufficient in principle to determine two of these unknowns, given the third. For this reason we are limited in the following discussion to placing constraints on the unknowns. The formation age of the zircons is assumed to be equal to the Pb–Pb age. This assumption has been tested for >4 Ga Jack Hills zircons and found to be generally valid (Harrison et al., 2006).

4. Pb–Pb and U–Xe discordancy and the inferred $(Pu/U)_o$

The previous data of Turner et al. (2004) hinted at a possible relationship between Pb–Pb and U–Pb discordancy and the loss of fissiogenic xenon implied by lower estimates of $(Pu/U)_o$. We now investigate the possibility of a similar relationship between the degree of discordancy between Pb–Pb ages and U–Xe ages and the estimates of $(Pu/U)_o$ obtained in the present work. The possibility of a relationship can be inferred by noting that a loss of xenon produces a lowered U–Xe age and, unless the loss occurred recently, a lowering of Pu/U. While there appears to be no obvious reason to expect a simple monotonic relationship, a general lowering of the projected $(Pu/U)_o$ ratio with increased discordancy is a reasonable expectation. In Fig. 2 $(Pu/U)_o$ is plotted as a function of the discordancy between Pb–Pb and U–Xe age for those data for which precise Pb–Pb ages have been determined. Aside from the high temperature release from zircon #12.12, there is indeed a general downward trend in the estimates of $(Pu/U)_o$ with increasing discordancy. For the most concordant samples (#1.4 and the major release from #12.12) the $(Pu/U)_o$ values cluster around 0.008 (mean 0.0077 ± 0.0006), i.e. close to the previously published chondritic value. In view of the possibility of Pu/U fractionation in various lithospheric processes preceding the crystallization of the zircon we do not feel it appropriate to place undue weight on this coincidence and certainly do not view it as necessarily providing support for the widely adopted chondritic value of Hudson et al. (1989) compared to other estimates (see the compilation by Azbel and Tolstikhin, 1993). What we do infer from the similarity with the 'chondritic' value is that the overall Pu/U fractionation associated with the genesis of the zircons is relatively small, of the order of a factor 2. Two interpretations for the high value (~0.015) for the high temperature release from zircon #12.12 suggest themselves: 1) the presence of a relict core, older by ~80 Ma than the measured Pb–Pb age would generate the necessary excess Pu–Xe, and 2) preferential partition by a factor of two of Pu relative to U into the zircon. The latter explanation is less likely however (unless it occurred in some premagmatic protolith), as it requires

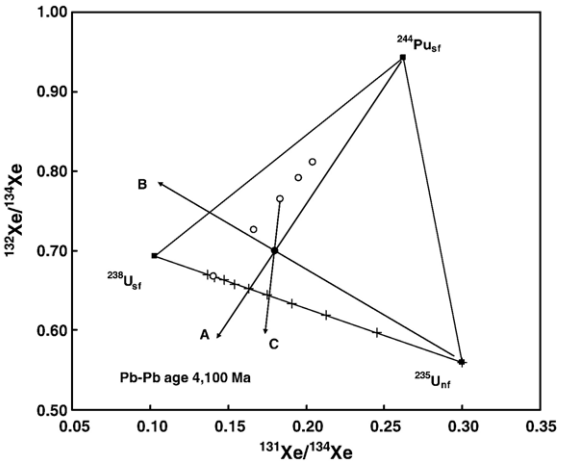

Fig. 4. Hypothetical example of a single datum from a partially outgassed 4100 Ma zircon. Projection A onto the ^{238}U–^{235}U join corresponds to a U–Xe age of 2500 Ma (crosses are at 500 Ma intervals counting from zero at the ^{235}U end member) but would only be a meaningful outgassing age if $(Pu/U)_o$ were infinite or very large (circles correspond to $(Pu/U)_o$ increasing in steps of 0.004 from zero on the ^{238}U–^{235}U join). Projection B onto the ^{244}Pu–^{238}U join corresponds to $(Pu/U)_o \sim 0.0035$ and would be a meaningful value only if the xenon loss occurred recently. Projection C represents the general case between these extremes and is arbitrarily drawn from a point corresponding to $(Pu/U)_o = 0.008$ to an outgassing age of ~2000 Ma.

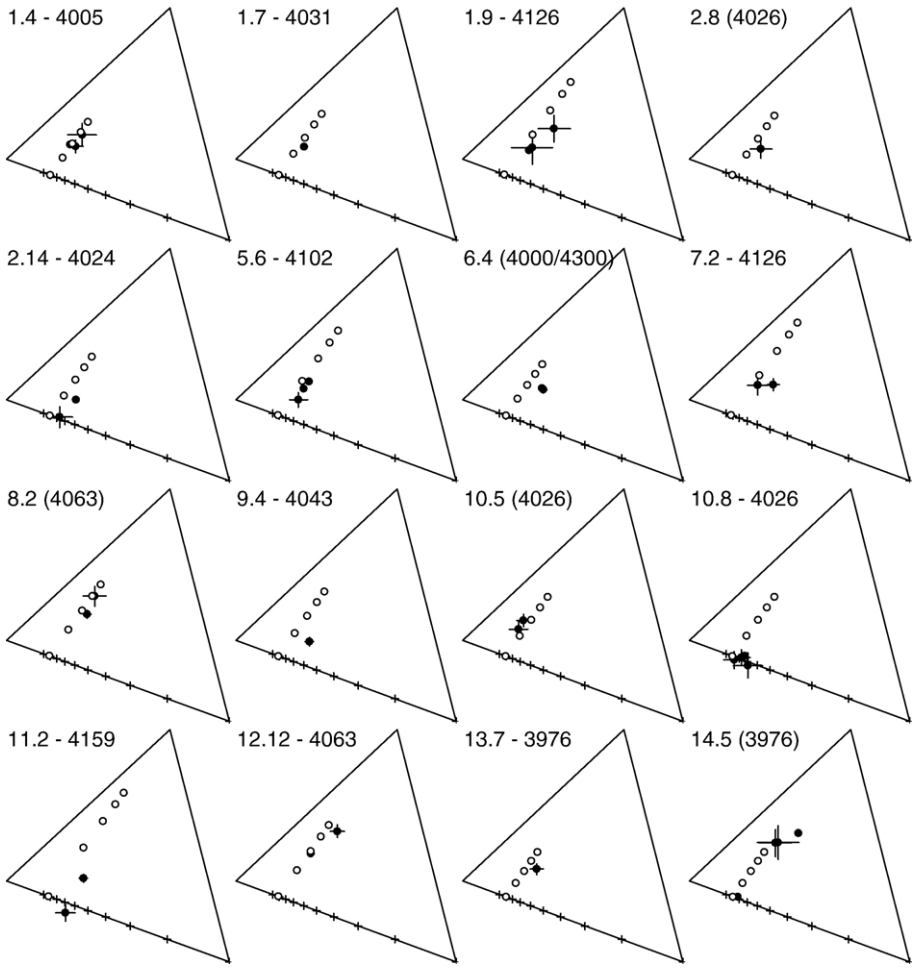

Fig. 5. Individual mixing triangles for the 16 zircons analysed. Axes have been removed for clarity. Crosses on the ^{238}U–^{235}U join correspond to U–Xe ages in increments of 500 Ma. Pb–Pb ages of individual zircons are indicated. Where these are uncertain (see text) they are shown in brackets. The circles correspond to $(Pu/U)_o$ ratios in increments of 0.004. Note how the positions of the circles along the line of concordancy depend strongly on the Pu decay between 4570 Ma and the indicated Pb–Pb age.

Pu/U fractionation in the opposite direction to that predicted by lattice strain parameters (Blundy and Wood, 2003).

5. Pu–U xenon ternary mixing diagram

We shall now consider in more detail how the ternary diagram may, in principle, be used to constrain the outgassing history and Pu/U ratios of the zircons.

5.1. Special case, the isochron plot

An interesting and informative special case arises where a group of coeval zircons, formed with identical Pu/U ratios at time t_1, have been subjected to varying degrees of partial xenon loss at a well defined time, t_2. The data on the ternary mixing diagram have the form of an isochron (Fig. 3). In the case where loss occurs after complete decay of ^{244}Pu, the isochron connects an intersection with the ^{244}Pu–^{238}U–^{235}U mixing line corresponding to the original formation age and Pu/U ratio, to a point on the ^{235}U–^{238}U 'timeline' corresponding to the time of loss. In the case where loss occurs when ^{244}Pu is still live, the isochron terminates at a point within the ^{244}Pu–^{238}U–^{235}U mixing triangle corresponding to the time of loss.

The hypothetical isochron plot described above would in principle permit a complete solution to the determination of Pu/U and the timing of xenon loss. Unfortunately the preconditions (coeval zircons with identical Pu/U) are unlikely to be satisfied by detrital zircons. In a few cases of samples with multiple releases, the data could conceivably lie on an isochron but are either not sufficiently precise or form a cluster. We are

therefore restricted to discussing the constraints imposed by single data points.

5.2. Pu–U xenon ternary mixing diagram: general case

Fig. 4 illustrates a hypothetical example corresponding to a single discordant datum from a 4100 Ma zircon. In the example the projection (A) from the Pu-fission point onto the 'age axis' corresponds to a U–Xe age of around 2500 Ma (symbols on the 'age axis' are at 500 Ma intervals, for this irradiation). This U–Xe 'age' would only be meaningful for $(Pu/U)_o$ infinite (or extremely high) which is thus unrealistic unless extreme Pu/U fractionation, favouring Pu, had occurred. The projection (B) from the ^{235}U n-fission point to the ^{238}U–^{244}Pu axis corresponds to $(Pu/U)_o \sim 0.0035$ (symbols on the 'concordia' line correspond to $(Pu/U)_o$ at intervals of 0.004). In general this represents a lower limit and would only equal the correct value for $(Pu/U)_o$ in the case where xenon loss had occurred recently, i.e. the data point lies on a zero age Pu–U–Xe isochron. A third line on Fig. 4 (C) corresponds to $(Pu/U)_o \sim 0.008$ and a U–Xe outgassing age of ~2000 Ma. This line is representative of the range of possible lines through the datum lying between the two extremes just referred to. Data for the individual zircons are shown in Fig. 5 together with the compositions expected for values of $(Pu/U)_o$ in increments of 0.004. Note on the individual plots how these compositions reflect the decay of ^{244}Pu between 4.57 Ga and the Pb–Pb formation age.

It is a simple matter to derive a relationship between the formation age, t_1, the outgassing age, t_2, the fraction of xenon produced from t_1 to t_2 remaining *after* the outgassing event, α, and $(Pu/U)_o$. Note that times are measured forward from solar system formation to the present day, for which we take T=4.57 Ga.

By definition:

$$\alpha = [\text{Xe (measured)} - \text{Xe (produced from } t_2 \text{ to } T)] \,/\, \text{Xe (produced from } t_1 \text{ to } t_2) \quad (1)$$

We also define:

$$R = (^{134}Xe_4)/(^{134}Xe_8) \quad (2)$$

and

$$F(t_i, t_j) = \text{B.Y.}[\exp(-\lambda t_i) - \exp(-\lambda t_j)] \quad (3)$$

where B is the branching ratio (fission/alpha decay), Y is the yield of ^{134}Xe per fission and the subscripts 4 an 8 refer to ^{244}Pu decay and ^{238}U decay respectively.

Thus α may be expressed as a function of t_1, t_2, T and the (present day) $^{134}Xe_8/^{238}U$ ratio used to calculate the U–Xe age,

$$\alpha = [(^{134}Xe_8/^{238}U).\exp(-\lambda_8 T) - F_8(t_2, T)]/F_8(t_1, t_2) \quad (4)$$

A further independent relationship between α, t_1 and t_2 is obtained by substituting expressions for xenon production from ^{244}Pu decay in expression Eq. (1). From this substitution and the definition of R we may then derive:

$$\alpha = [R.F_8(t_2,T) - (Pu/U)_o.\ F_4(t_2, T)]/[(Pu/U)_o.\ F_4(t_1, t_2) - R\ .\ F_8(t_1, t_2)] \quad (5)$$

The relationships between α and t given by expressions (4) and (5) are shown in Fig. 6 for $(Pu/U)_o$=0.008 and t_1=4200 Ma.

The corresponding plot for zircons with discordant Pb–Pb and U–Xe ages is shown in Fig. 7 for $(Pu/U)_o$=0.008. It is clear from the figure that partial xenon loss has occurred for these zircons and at different times for different zircons. The zircons were extracted from the same ca. 3 Ga metaquartzite and thus are expected to have experienced relatively similar thermal histories since that time. Their unknown and likely differing thermal histories are permissive of highly variable xenon loss occurring prior to deposition. Based solely on the U–Xe ages this

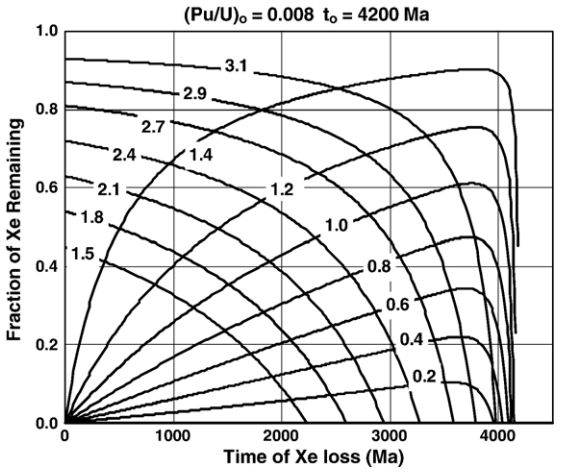

Fig. 6. Example of a single stage outgassing model relating time of xenon loss and fraction of xenon remaining after outgassing for the case $(Pu/U)_o$=0.008 and a formation age of 4200 Ma. The curves show: (1) present day $^{134}Xe_8/U$ ratios (1.5 to 3.1) in units of 10^{-8}, and (2) $^{134}Xe_4/^{134}Xe_8$ ratios for fissiogenic xenon from ^{244}Pu and ^{238}U respectively (0.2 to 1.4).

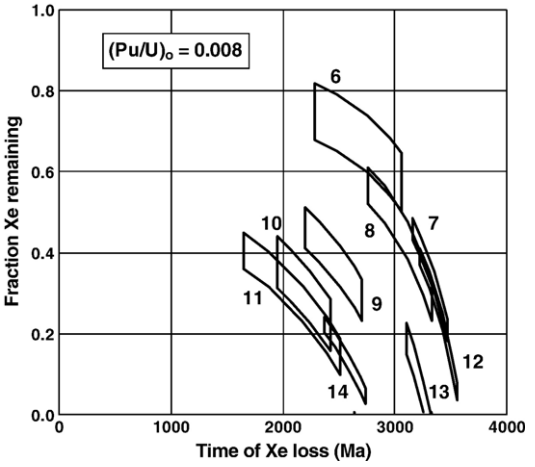

Fig. 7. Single stage outgassing model relating time of xenon loss and fraction of xenon remaining after outgassing for the actual zircon data, assuming $(Pu/U)_o = 0.008$ and Pb–Pb ages as measured. Key to sample numbers and temperature steps in Table 1: 6—1.7(13.5), 7—5.6(13), 8—5.6(14), 9—2.14(12.5), 10—9.4(13), 11—7.2(12), 12—1.9(13), 13—10.8(12), 14—11.2(13) same as Fig 2.

explanation would represent a possibility as the youngest U–Xe age is not demonstrably younger than deposition. However the presence of Pu–xenon in zircons with young U–Xe ages and its implications, exemplified by Fig. 7, suggest that, in some cases at least, xenon loss occurred after 3 Ga. Xenon transport is very sluggish under crustal conditions (Honda et al., 2003) and if some loss did occur after deposition it is most likely due to non-thermal causes such as mineralogical degradation due to metamictization (Krogh, 1982). A way around this conclusion, theoretically, would be if $(Pu/U)_o$ were very high in zircons 2.14, 7.2, 9.4, and 11.2.

6. Summary and discussion

We have confirmed earlier evidence for the former presence of live ^{244}Pu in ancient detrital zircons from Western Australia and devised a procedure for investigating the effects of xenon loss on inferred Pu/U ratios. We have shown how a ternary mixing diagram of $^{132}Xe/^{134}Xe$ vs. $^{131}Xe/^{134}Xe$ for neutron irradiated zircons can be used to determine both Pu/U ratios and U–Xe spontaneous fission ages. U–Xe ages are typically lower than the Pb–Pb ages indicating that xenon loss is common. Retention of ^{244}Pu xenon when loss occurred subsequent to Pu decay implies that xenon loss was incomplete and consequently U–Xe ages are higher than the actual time of loss. We have demonstrated how the ternary diagram can be interpreted to place constraints on the timing and extent of the loss and in principle to generate a xenon loss isochron. Variable xenon loss appears, in some cases, to be the result of metamictization rather than differing thermal histories. Inferred $(Pu/U)_o$ ratios show a general decrease with the increase in discordancy between Pb–Pb and U–Xe ages. For the least discordant samples we infer $(Pu/U)_o \sim 0.008$ which is close to the published meteorite values.

Fractionation of Pu and U may occur in the protolith of the magma, during melt formation and in the crystallisation from the melt. Some of the variability in estimates of $(Pu/U)_o$ may arise from this in addition to xenon loss. It has been suggested from O-isotope measurements that the protolith of some zircons may have been sediments which acquired elevated $^{18}O/^{16}O$ ratios from interactions with an early hydrosphere. Since we do not have O-isotope data for the zircons analysed in this study we can add little to arguments for or against this hypothesis beyond noting the absence of major (i.e. greater than a factor 2) Pu–U fractionation in our data, which could have resulted from aqueous interactions. Furthermore, the absence of major Pu–U fractionation during zircon crystallisation is probably an indication that both behave compatibly, being incorporated into the zircon structure in the 4+ valence state. The behaviour of Pu and U contrasts strongly with that of the trivalent rare earth elements which are strongly depleted. This is particularly so for the light rare earths, for which Nd/U ratios are depleted by 3 or 4 orders of magnitude compared to chondritic values.

For the reasons just discussed it is not possible to argue that the value of $(Pu/U)_o$ inferred from zircons is more, or less, applicable to the solar system as a whole than the widely used meteoritic values. Estimates of $(Pu/U)_o$ from measurements on achondrites (e.g. Lugmair and Marti, 1977) are based on similarity in the geochemical behaviour of Pu and Nd in merrillite and are subject to the same uncertainties surrounding magma generation that we have alluded to for zircons. The approximate self consistency of Pu/Nd ratios used in attempts to construct a ^{244}Pu time scale for achondrites (Shukolyukov and Begemann, 1996) does not preclude a systematic difference between the achondritic and average solar system values. The widely used chondritic value is potentially more representative of average solar system but is arguably less certain than the quoted experimental error. The bulk $(Pu/U)_o$ ratio, inferred from two samples of St Severin (LL6), is based on combining temperature steps which show a factor 4 variation in Pu/U and then applying decay corrections based on whole rock I–Xe ages. We believe there is a case for revisiting the chondritic system with a view to obtaining a more comprehensive understanding of the internal and external

variability of Pu/U. There is also a case for applying the techniques of the present study to zircons with raised $^{18}O/^{16}O$ ratios.

Acknowledgements

This work was supported by grants from PPARC (AB), NERC (SC), the Australian Research Council (TMH) and NASA Exobiology Program (SJM). We also wish to thank Dave Blagburn and Bev Clementson for technical assistance throughout the project.

References

Azbel, I.Y., Tolstikhin, I.N., 1993. Accretion and early degassing of the Earth: constraints from Pu–U–I–Xe isotopic systematics. Meteoritics 28, 609–621.

Blundy, J., Wood, B., 2003. Mineral-melt partitioning of uranium, thorium and their daughters. Rev. Mineral. Geochem. 52, 59–123.

Clayton, D.D., 1983. Extinct Radioactivities — A 3-Phase Mixing Model. Astrophys. J. 268, 381–384.

Gilmour, J.D., Lyon, I.C., Johnston, W.A., Turner, G., 1994. RELAX: an ultrasensitive, resonance ionization mass spectrometer for xenon. Rev. Sci. Instrum. 65, 617–625.

Harrison, T.M., McCulloch, M.T., Blichert-Toft, J., Albarede, F., Holden, P., Mojzsis, S.J., 2006. Further Hf isotope evidence for Hadean continental crust. Geochim. Cosmochim. Acta 70, A234 (Suppl).

Hebeda, E.H., Freudel, M., Shultz, L., 1987. Radiogenic, fissiogenic and nucleogenic noble gases in zircons. Earth Planet. Sci. Lett. 85, 79–90.

Honda, M., Nutman, A.P., Bennett, V.C., 2003. Xenon compositions of magmatic zircons in 3.64 and 3.81 Ga meta-granitoids from Greenland — a search for extinct Pu-244 in ancient terrestrial rocks. Earth Planet. Sci. Lett. 207, 69–82.

Hudson, G.B., Kennedy, B.M., Podosek, F.A., Hohenberg, C.M., 1989. The Early Solar System Abundance of (super 244) Pu as inferred from the St. Severin Chondrite, 19th Lunar and Planetary Science Conference, pp. 547–557.

Krogh, T.E., 1982. Improved Accuracy Of U–Pb Zircon Ages By The Creation Of More Concordant Systems Using An Air Abrasion Technique. Geochim. Cosmochim. Acta 46, 637–649.

Krylov, D.P., Meshick, A.P., Shukolyukov, Y.A., 1993. The zircon Xe_s–Xe_n spectrum dating of primary events in high-grade metamorphic terrains — the example of Archaean Napier Complex (East Antarctica). Geochem. J. 27, 91–102.

Kunz, J., Staudacher, T., Allègre, C.J., 1998. Plutonium-fission xenon found in Earth's mantle. Science 280, 877–880.

Lugmair, G.W., Marti, K., 1977. Sm–Nd–Pu time-pieces in Angra–Dos–Reis meteorite. Earth Planet. Sci. Lett. 35, 273–284.

Meyer, B.S., Clayton, D.D., 2000. Short-lived radioactivities and the birth of the Sun. Space Sci. Rev. 92, 133–152.

O'Nions, R.K., Tolstikhin, I.N., 1994. Behavior and residence times of lithophile and rare-gas tracers in the upper-mantle. Earth Planet. Sci. Lett. 124, 131–138.

Peck, W.H., Valley, J.W., Wilde, S.A., Graham, C.M., 2001. Oxygen isotope ratios and rare earth elements in 3.3 to 4.4 Ga zircons: ion microprobe evidence for high delta O-18 continental crust and oceans in the Early Archean. Geochim. Cosmochim. Acta 65, 4215–4229.

Porcelli, D., Wasserburg, G.J., 1995. Mass-transfer of helium, neon, argon, and xenon through a steady-state upper-mantle. Geochim. Cosmochim. Acta 59, 4921–4937.

Shukolyukov, A., Begemann, F., 1996. Pu–Xe ages of eucrites. Geochim. Cosmochim. Acta 60, 2453–2471.

Shukolyukov, Y., Kirsten, T., Jessberger, E.K., 1974. The Xe–Xe spectrum technique, a new dating method. Earth Planet. Sci. Lett. 24, 271–281.

Staudacher, T., Allègre, C.J., 1982. Terrestrial xenology. Earth Planet. Sci. Lett. 60, 389–406.

Teitsma, A., Clarke, W.B., Allègre, C.J., 1975. Spontaneous fission-neutron fission xenon: a new technique for dating geological events. Science 189, 878–880.

Turner, G., Harrison, T.M., Holland, G., Mojzsis, S.J., Gilmour, J., 2004. Extinct Pu-244 in ancient zircons. Science 306, 89–91.

Turner, G., Gilmour, J., Crowther, S., Busfield, A., Mojzsis, S., Harrison, M., 2005. Extinct plutonium geochemistry of ancient hadean zircons. Eos Trans. AGU 86 Fall Meet. Suppl., Abstract V21F-05.

Wasserburg, G.J., Busso, M., Gallino, R., 1996. Abundances of actinides and short-lived nonactinides in the interstellar medium: diverse supernova sources for the r-processes. Astrophys. J. 466, L109–L113.